J. Eng. Technol. Sci., Vol. 53, No. 1, 2021, 210111

Bond Strength Behavior for Deformed Steel Rebar Embedded in Recycled Aggregate Concrete

Aseel Abdulazeeza*, Raad Abdulkhudhur & Hussein Al-Quraishi

Structural Engineering Division, Faculty of Civil Engineering, University of Technology, Alsenaa Street, Iraq
*E-mail: 11608@uotechnology.edu.iq

Highlights:

- Studying the effect of bar size, embedded length, replacement ratio of RCA, concrete cover and yield stress of a reinforcing bar on its bond strength in RAC through an experimental program.
- Providing a wide range of bank data for the most effective variables through a parametric study on numerical analysis.
- Proposing a new design equation to predict the bond strength between the reinforcing bar and the surrounding RAC.

Abstract. This study investigated the bond strength behavior of a deformed steel bar embedded in RAC through an experimental program and numerical analysis. In the experimental work, eighteen push-out specimens were tested. The compressive strength of RAC, the recycled aggregate replacement ratio, the embedded length of the reinforcing bar, the size of the rebar, the concrete cover, and the yield stress of the reinforcing steel bar were the main parameters investigated. The effect of these parameters on bond strength, bond-slip behavior, and modes of failure are discussed. Analysis of the test results indicate that the bond strength in concrete is reduced by 13% when using a specimen constructed from recycled aggregate compared with conventional concrete. The failure modes in a reinforcing bar embedded in RAC representing splitting failure and push-out failure, were similar to those in conventional concrete. The finite element analysis presented in this study was used to analyze forty-four push-out specimens. Through numerical analysis, the bond strength of RAC was related to the 0.57 power function of compressive strength. A design equation for bond strength of reinforcing bars embedded in RAC is proposed. The proposed equation was calibrated through the numerical and experimental results.

Keywords: *bond strength; experimental work; finite element analysis; proposed design equation; recycled aggregate concrete.*

1 Introduction

Approximately 48 billion tons of natural coarse aggregate are consumed every year in construction of the concrete structures. At the same time, the amount of construction waste increases through demolishing old buildings, which is a real

Received April 24th, 2020, 1st Revision September 8th, 2020, 2nd Revision October 19th, 2020, 3rd Revision November 16th, 2020, Accepted for publication November 19th, 2020.
 ISSN: 2337-5779,
DOI: 10.5614/j.eng.technol.sci.2021.53.1.11

concern for the environment. The waste from demolishing concrete structures reaches up to 850 tons in Europe every year, because of the shortage of landfills [1]. Using of recycled aggregate concrete (RAC) can help solve this problem and remove negative environmental impacts. The presence of old adhered mortar and the high absorption affect the mechanical properties and durability of RAC, because of which it has lower quality compared to natural aggregate concrete (NAC) [2].

The structural performance of reinforced concrete is affected by the bond between the steel bars and the surrounding concrete. The bond strength depends on many variables, such as the diameter of the rebar, the compressive strength of the concrete, the concrete cover, the embedded length, the yield stress of the steel bar, the presence of lateral reinforcement, and the position of the rebar [3].

Numerous studies have been carried out on the bond strength between rebar and surrounding concrete constructed from natural aggregate, however, relatively a few studies have investigated the bond characteristics between rebar and RAC [4]. Alhawat and Ashour [5] investigated the bond strength of 60 RCA specimens with corroded and uncorroded rebar with the following parameters: bar diameter, RCA content, embedded length and corrosion level. The test result showed there was a slight effect on bond strength when using RCA compared with NAC. Arezoumandi, *et al.* [6] studied the effect of the replacement ratio on bond strength between rebar and surrounding concrete with 50% and 100% replacement ratios as replacement level in RAC. Eighteen pull-out specimens and nine full-scale beams were tested to evaluate the bond strength. The results showed that replacing more than 50% of the natural aggregate reduced the bond strength compared with the virgin natural aggregate specimens. Also, the splice length equation according to ACI 318-14 needs to be modified so as to be applicable to RAC beams. Butler, *et al.* [7] studied the effect of different replacement ratios on the bond strength of reinforcing bars embedded in RAC. Beam-end specimens were tested to find the bond strength of reinforcing bars embedded in RAC. The test results indicated that the bond strength of specimens that contain natural aggregate was greater than the bond strength of specimens with RAC by 9% to 19%.

Dong, *et al.* [8] investigated the bond behavior of reinforcing bars embedded in RAC under flexural action by testing fifteen beams. The considered variables were the recycled fine aggregate replacement ratio, the water-binder ratio, the recycled aggregate replacement ratio, the reinforcement anchorage length and the bar surface shape. The bond-slip behavior and ultimate bond strength were recorded. The test results showed that the bond strength decreased with an increase of the replacement ratio of RCA. Further, the bond strength between the RAC and the reinforcing bar was two times of that of a plain reinforcement. Also, increasing the anchorage length led to a decrease in the bond strength. Fernandez, *et al.* [9] studied the bond behavior between reinforcing rebar and surrounding concrete in RAC specimens. The replacement ratios in RA were 20%, 50% and 100%, obtained from demolishing old concrete with 40 MPa compressive strength. The ultimate bond strengths of the corroded and the uncorroded rebar were presented.

Kim, *et al.* [10] investigated the bond strength of rebar in RAC. The main variables considered were: the replacement ratio of recycled aggregate and the water to cement ratio of the concrete mixture. The test results indicated that the bond splitting strength was affected by the roundness of the recycled aggregate and the weak interfacial transition zone between the recycled aggregate and the cement paste, which has a more porous structure. Further, a linear function between the density of RAC and bond strength was found. A multivariable model using regression analysis was developed to predict the bond strength in RAC. Also, it was found that the code of practice is very conservative in predicting the bond strength of RAC.

Pandurangan, *et al.* [11] compared the effect of different treatments of RAC on bond strength, i.e. acid treatment, mechanical treatment and thermal treatment. Fifteen RILEM beams were constructed from a natural aggregate, recycled treated aggregate with acid, and thermal and recycled untreated aggregate. The treatment of RA using thermal mechanical and acid improved the physical properties of the RAC. The acid treatment was more effective in improving the bond strength. Prince, *et al.* [12] tested 24 spliced beams to predict the splice strength of reinforcing bars embedded in RAC under four-point load, concrete grade, RAC replacement ratio, rebar diameter and rebar surface properties. The test result showed that the bond behavior and the modes of failure of the NAC and the RAC were similar. The regression analysis of the experimental test results showed a 1/4 power function representative of the compressive strength of the RAC. The ACI 408R-03 equation was relatively accurate for predicting the bond strength of the RAC.

Hamad, *et al.* [13] tested reinforced concrete beams with different RAC replacement ratios. The percentages of replacement were 0%, 40% and 100% and the modes of failure were shear, flexural and splitting bond. The experimental program results showed that there were small differences between the ultimate load and the load-deflection behavior of the RAC and the NAC. The results were compared with ACI provisions and previous researches. Also, validation of the experimental work was done using finite element analysis and both results were compared. Pour and Alam [14], investigated the bond strength behavior in RAC by testing 144 push-out specimens. 0%, 30%, 40% and 50% were the RCA replacement ratios used in producing the specimens. The embedded length and concrete cover were the variables considered. It was concluded that an increase in embedded length and bar diameter produced a reduction in bond strength. Similar to the case of conventional concrete, increasing the concrete cover improved the bond strength. Further, a new formula for predicting the bond strength based on the test results was proposed.

In summary, it can been noted that limited test results and a small range of variables data that effect the bond strength of RAC were used in predicting the proposed equation. Further, relatively few numerical analyses of bond strength of RAC were carried out. Therefore, the main objectives of the present study were: 1) to study the effect of bar size, embedded length, RCA replacement ratio, concrete cover and rebar yield stress on the bond strength of rebar in RAC through an experimental program; 2) to provide a wide range of bank data for the most effective variables through a parametric study on numerical analysis. And finally, 3) to propose a new design equation to predict the bond strength between rebar and surrounding RAC.

2 Experimental Program

2.1 Materials

The materials used in this work were Portland cement (type I), natural coarse aggregate with a maximum size of 20 mm, fine aggregate, recycled coarse aggregate produced from demolishing old reinforced concrete columns available in the Material Laboratory at the University of Technology, Iraq. The crushed concrete had a compressive strength between 25 to 30 MPa at one year age. It was washed and then sieved in accordance with ASTM C33 [15]. Table 1 shows the physical properties of the aggregate used in the present study. Four deformed bars with a size of 12, 16, 22, and 25 mm were used in constructing the specimens.

Table 1 Physical properties of aggregate.

Physical properties	Natural fine aggregate	Natural coarse aggregate	Coarse recycled aggregate
Maximum grain size (mm)	5	20	20
specific density	2.60	2.63	2.50
Water absorption (%)	2.10	1.03	4.40
Bulk density (kg/m^3)	1590	1610	1370

2.2 Specimen Details

According to the RILEM CEB/FIP [16], the dimensions of the tested specimens were adopted. Eighteen push-out specimens were constructed. The shape of the specimens was cubic, with dimensions of 150 x 150 x 150 mm. A single deformed steel bar was embedded with a short anchorage length in the center of the cubic.

This small anchorage was between 5D to 12D in diameter, which represents the bonding length and provide a uniform stress along the embedded length. The anchorage length was located in the middle, while the upper part or lower part of the specimen was debonded by using a 2.5D PVC pipe, see Figure 1.

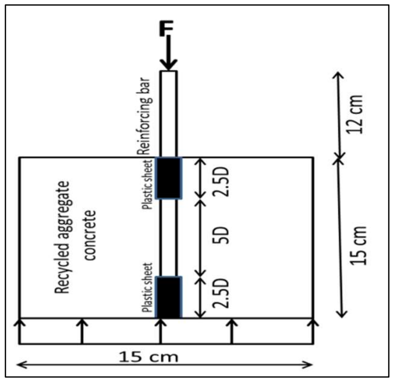

Figure 1 Tested specimen details.

2.3 Concrete Mix Design, Casting and Curing

The absolute volume method was used to design the NAC, while the equivalent mix proportion method was used to design the RAC. The natural aggregate was replaced with the recycled aggregate by a percentage of 50% and 100%. Six trail mixes for the target compressive strengths of 15, 25, 35, and 50 MPa for RAC and 25 MPa for NAC were adopted after 28 days. The details of the mix proportions are presented in Table 2.

After casting the concrete, the specimens were demolded after 24 h. Then, to cure the specimens placed in a water tank for 28 days.

Table 2 Mix proportions.

f_c (MPa)	Type of concrete	Replacement ratio (%)	Cement (kg)	Sand (kg)	Aggregate (kg)	Water (kg)	Water/cement ratio
	NAC	0	360	757	1057	184	0.51
25	RAC	50	373	757	1057	198	0.53
	RAC	100	382	757	1057	210	0.55
15	RAC	100	305	775	1080	186	0.61
35	RAC	100	415	714	1024	166	0.40
50	RAC	100	525	637	913	205	0.39

2.4 Testing the Specimens According to the Considered Variables

A total of 18 specimens divided into 6 groups were constructed from the natural and recycled aggregate to study the bond strength behavior between the reinforcing bar and the surrounding recycled aggregate concrete. The variables considered in this study were natural aggregate replacement ratio (group one in Figure 2(a)), the compressive strength of RAC (group two in Figure 2(b)), the diameter of the rebar (group three in Figure 2(c)), the embedded length of the rebar (group four in Figure 2(d)), the yield stress of the rebar (group 5 in Figure 2(e)) and finally the concrete cover (group 6 in Figure 2(f)).

The details of the experimental program were as follows: the replacement ratio effect on bond strength was studied for 3 specimens (P3-Rep0%, P2-Rep50%, and P1-Rep100%). The compressive strength of RAC was investigated by comparing 4 specimens (P1-Rep100%, P4-fc15, P5-fc35, and P6-fc50). The effect of the diameter of the bar was studied by comparing 4 specimens (P1-Rep100%, P7-D16, P8-D22, and P9-D25). The embedded length of the rebar in RAC was investigated by comparing 4 specimens (P1-Rep100%, P10-Em7D, P11-Em10D, and P12-Em12D). The yield stress of the rebar was studied by comparing 4 specimens (P1-Rep100%, P13-fy325, P14-fy420, and P15-fy625). The effect of concrete cover was investigated by comparing 4 specimens (P1-Rep100%, P16-Co100, P17-Co200, and P18-Co250). The characteristics of the tested specimens are listed in Table 3.

Table 3 Characteristics of tested specimens.

Group	Specimen	Replacement ratio (%)	f_c (MPa)	Bar size (mm)	Embedded length (mm)	Yield stress of rebar	Concrete cover (mm)
Reference	P1-Rep100%	0	25	12	5D	525	150
Group 1	P2-Rep50%	50	25	12	5D	525	150
	P3-Rep0%	100	25	12	5D	525	150
Group 2	P4-fc15	100	15	12	5D	525	150
	P5-fc35	100	35	12	5D	525	150
	P6-fc50	100	50	12	5D	525	150
Group 3	P7-D16	100	25	16	5D	525	150
	P8-D22	100	25	22	5D	525	150
	P9-D25	100	25	25	5D	525	150
Group 4	P10-Em7D	100	25	12	7D	525	150
	P11-Em10D	100	25	12	10D	525	150
	P12-Em12D	100	25	12	12D	525	150
Group 5	P13-fy325	100	25	12	5D	325	150
	P14-fy420	100	25	12	5D	420	150
	P15-fy625	100	25	12	5D	625	150
Group 6	P16-Co100	100	25	12	5D	525	100
	P17-Co200	100	25	12	5D	525	200
	P18-Co250	100	25	12	5D	525	250

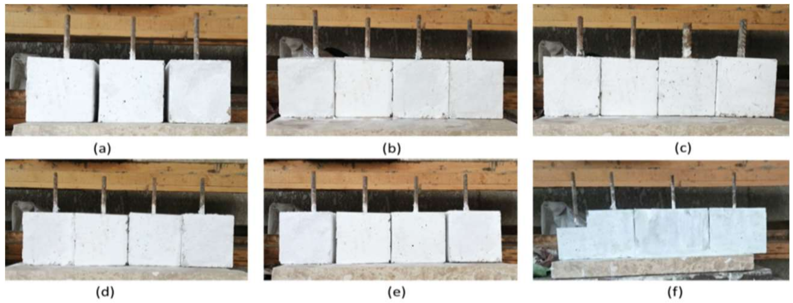

Figure 2 The tested specimen groups: (a) group 1, (b) group 2, (c) group 3, (d) group 4, (e) group 5 and (f) group 6.

2.5 Testing Procedure

Push-out testing was conducted for both the RAC and the NAC specimens using a hydraulic machine of 120 kN capacity. In this test, the reinforcing bar is pushed downward from one end to produce slip between the RAC and the reinforcing bar. The test was carried out using a displacement control of 0.1 mm/min. Steel blocks with holes were placed under the RAC specimens during the process of applying compression force at the other end of the specimens. At the end of the reinforcing bar, the slippage (vertical displacement) was recorded using the displacement of the actuator. Figure 3 shows the specimen under testing.

Figure 3 The specimens under testing.

3 Experimental Results

The ultimate bond strength was assumed to be uniformly distributed along the anchorage length of the reinforcing bar in the RAC. It can be calculated according to Eq. (1):

$$\tau_{ult} = P_{ult} / (\pi D * l_d) \quad (1)$$

where τ_{ult} is the ultimate bond stress; P_{ult} is the ultimate applied force; D is the nominal diameter of the steel bar and l_d is the embedded length of the reinforcing bar in the RAC.

3.1 Variables Effect on Bond Strength

The influence of the considered variables on the bond strength are shown in Table 4 and can be summarized as follows. Increasing the replacement ratios of natural aggregate by recycled aggregate from 0% to 100% decreased the bond stress by 13%. This was due to the reduction of the adhesive force and mechanical interlock through the presence of micro-cracks in the RCA surface. This is in agreement with the results obtained by Alhawat and Ashour [1]. As expected, increasing the compressive strength of the RAC from 15 to 50 Mpa increased the bond strength by 107.7%. This confirms the major role of RAC compressive strength on bond strength, which is in agreement with the results obtained by Fernandez, *et al.* [5]. The bond strength of the reinforcing bar embedded in the RAC was decreased by 52.2% when the diameter of the steel reinforcing bar was increased from 12 to 25 mm. This can be attributed to the increase in the amount of bleed water trapped between the concrete and the steel bar surface, which consequently increased the voids and reduced the contact surface area and then reduced the bond strength. In addition to that, the number of ribs was reduced when the steel bar diameter was increased. This also may be the reason behind the reduction of the bond strength. It is in agreement with the test results obtained by Alhawat and Ashour [1]. Increasing the embedded length of the reinforcing bar in the RAC from 5D to 12D decreased the bond strength by 16.3%. This was mainly due to the small amount of bond stress distributed along the bar when the embedded length was increased. This is in agreement with the test results obtained by Alhawat and Ashour [1].

The bond strength between the RAC and the reinforcing bar increased by 131.9% when the yield stress of the reinforcing bar was increased from 325 to 625 MPa. This was due to the increase of the circumference stresses transferred between the steel bar and the surrounding concrete when the yield stress increased. When the RAC cover was increased from 100 to 250 mm the bond strength increased by 3%. The likely reason for this is the confinement effect produced by the concrete cover.

Table 4 Ultimate bond strength.

Group	Specimens	Ultimate bond stress (MPa)
Reference	P1-Rep100%	10.40
Group 1	P2-Rep50%	11.12
	P3-Rep0%	11.96
Group 2	P4-fc15	6.10
	P5-fc35	10.81
	P6-fc50	12.67
Group 3	P7-D16	7.79
	P8-D22	5.65
	P9-D25	4.97
Group 4	P10-Em7 Ø	10.11
	P11-Em10 Ø	9.12
	P12-Em12 Ø	8.79
Group 5	P13-fy325	9.81
	P14-fy420	13.82
	P15-fy625	22.78
Group 6	P16-Co100	9.88
	P17-Co200	10.03
	P18-Co250	10.10

3.2 Bond Stress-Slip Relations

The bond stress is calculated by dividing the applied force over the RAC contact surface area. The slip between the reinforcing bar and the surrounding concrete is recorded using the testing machine displacement control. The bond strength-slip behavior of the RAC and the NAC showed similar patterns. Figure 4 shows the three stages of the bond stress-slip response of the push-out specimens. In the first stage, the curve ascends up to approximately 91% of the ultimate bond stress. In this stage, the chemical adhesion was predominant. Next, nonlinear behavior of the bond stress-slip occurred until the peak stress was reached. The mechanical interlock contributed to the bond stress in this stage. In the third stage, the curve descends approximately linearly until failure occurred.

3.3 Modes of Failure

Bond failure in RAC specimens starts with friction and adhesion failure, which represents the linear zone of the bond-slip behavior. The real bond strength begins at the nonlinear part of the bond stress-slip behavior. At this stage, maximum radial tensile stresses perpendicular to the axial force direction in the reinforcing bar are created. Surface cracks in the softening zone of the bond stress-slip behavior occur after the radial stresses reach the maximum tensile strength of the RAC. Therefore, two types of failure occurred in the push-out test: splitting failure occurred due to the radial tensile stress as indicated above; and push-out failure occurred when the partial shear key between the two ribs caused to push out the reinforcing bar to the other side without exterior cracks. When the replacement ratio of the natural aggregate is increased, the compressive strength of the RAC increases the bar diameter, the yield stress of reinforcing bar leads to a splitting type of failure along with increased the crack width on the surface of the concrete. Meanwhile, increasing the concrete cover led to a push-out type of failure with a small concrete crack at the surface, see Figure 5.

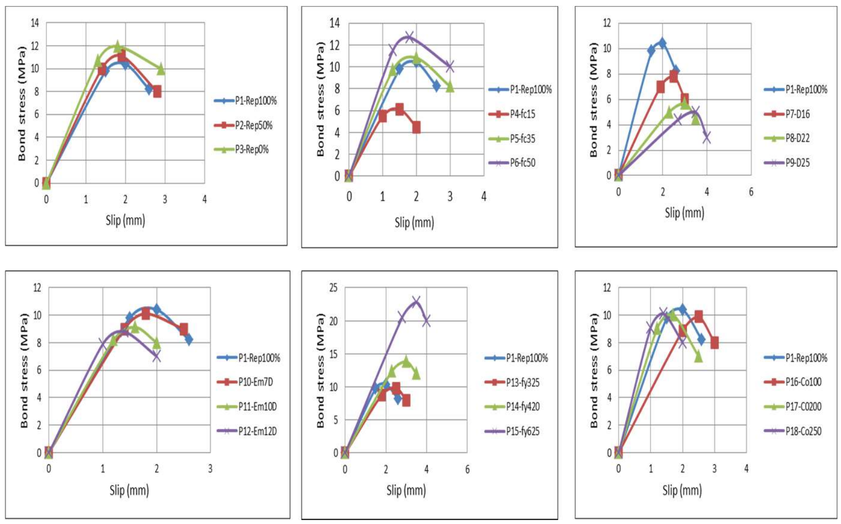

Figure 4 Bond stress-slip behavior of tested specimens.

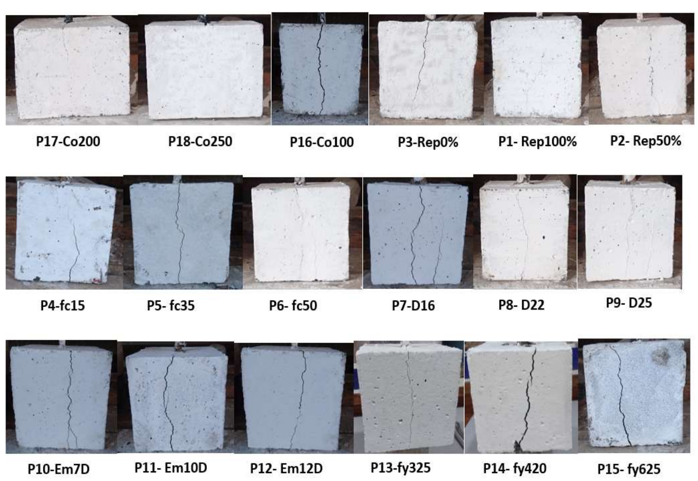

Figure 5 Modes of failure of the tested specimens.

4 Numerical Analysis

The ABAQUS software program, version 6.14 [17] was used to simulate the bond behavior of the RAC specimens that were experimentally tested. The material and geometrical modeling in ABAQUS are discussed in the following subsections.

4.1 Materials Modeling

Concrete damage plasticity was the material model adopted in the numerical analysis. This model uses the isotropic damage elasticity in combination with isotropic tensile and compressive plasticity to describe the inelastic behavior of concrete. Further, the model combines the multi-hardening plasticity and isotropic damage elasticity to represent irreversible damage during the fracture of concrete.

In ABAQUS, the cracking in concrete is simulated using smeared cracks in the element or a discrete crack model in the node of the element. The smeared crack model with a fixed direction was adopted.

The linear elastic-perfect plastic law was used to model the steel reinforcing bar. The nonlinear equation was solved using the Newton Raphson method with load increments of 0.1 kN.

4.2 Geometry Modeling

The geometry simulation of the push-out specimen was carried out using 3D isoparametric elements with 16 nodes. A brick element of size 0.1 x 0.1 x 0.1 cm was used to represent the whole specimen. Figure 6 shows the simulation geometry of the push-out specimens.

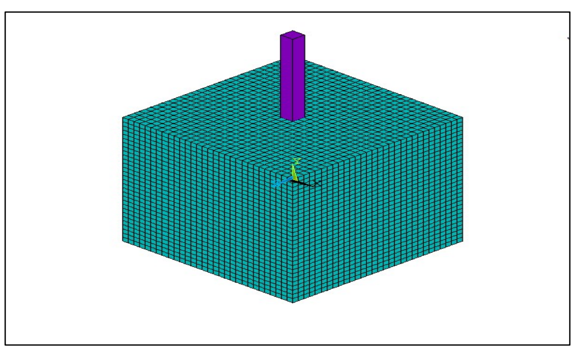

Figure 6 Numerical simulation of the push-out specimens.

4.3 Bond-Slip Law in ABAQUS

The experimental bond stress-slip relationship presented in this study for the reference specimen was used in ABAQUS. Table 5 shows the values of the bond stress and slip used in the numerical analysis.

Table 5 Bond stress-slip behavior.

Bond stress (MPa)	Slip (mm)
0	0
9.8	1.5
10.4	2
8.2	2.6

4.4 Calibration of the Numerical Model

The selected geometrical and material model in ABAQUS must be verified through comparisons with the experimental load deflection curves. Verification was carried out on one specimen for each variable. From Figure 7, the ratio between the numerical and the experimental ultimate bond stress had an average of 0.91. Moreover, the numerical load-deflection curve captured the experimental one, which consequently gave an accurate adopted numerical model.

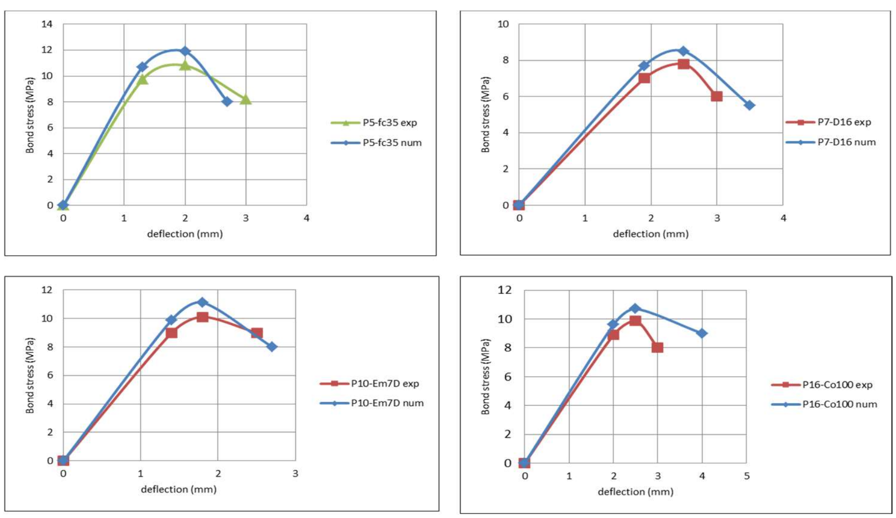

Figure 7 Numerical and experimental load-deflection curves.

4.5 Parametric Study

A wide range of bank data through a parametric study of the verified FE model was collected. This parametric study helps to describe the effect function for each variable, in addition to providing a wide range of data to propose a design equation of the bond strength of the reinforcing bar embedded in the RAC.

The 44 four push-out specimens were analyzed numerically to predict the bond strength for the following ranges of values of the variables: from 15 MPa to 55 MPa for the compressive strength of the RAC; from 10 mm to 42 mm for the diameter of the reinforcing bar; from 25 to 600 mm for the anchorage length of the reinforcing bar; and finally from 150 mm to 500 mm for the concrete cover.

From Figure 8 it can be seen that:

1. Nine specimens were numerically analyzed to study the effect of the compressive strength of the RAC on the bond strength with values ranging between 15 and 55 MPa. From Figure 8(a) it can be seen that there was an increase in the bond stress with a power function of 0.57 along with increasing compressive strength.
2. Seventeen specimens were numerically analyzed with the bar diameter ranging between 10 mm and 42 mm to study the effect of rebar size on the bond stress. From Figure 8(b) it can be seen that there was a proportional decrease of the bond stress with a power function of 1.0 due to the relationship between bond strength and reinforcing bar diameter.
3. Nine specimens with anchorage length varying from 25 to 600 mm were numerically analyzed to study the effect of the embedded length on the bond strength. Figure 8(c) shows that the bond stress decreased linearly along with an increase of the embedded length.
4. Nine specimens were numerically analyzed to study the effect of the concrete cover, ranging from 100 mm to 500 mm, on the bond strength. Figure 8(d) shows that the bond stress increased with a power function of 0.03.

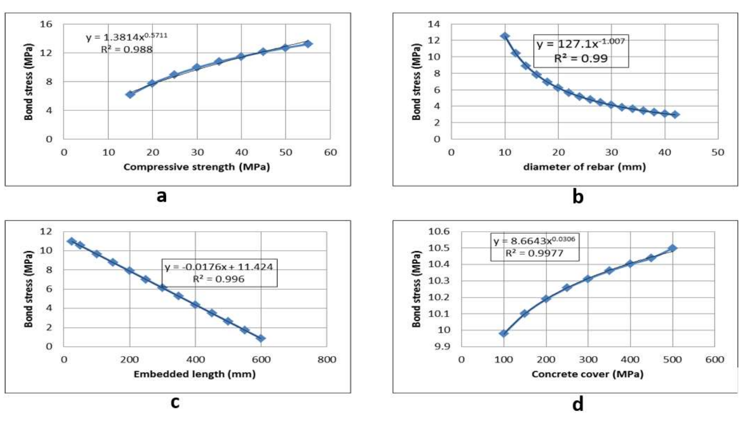

Figure 8 Parametric study.

5 Proposed Design Equation

In order to propose the bond strength equation for RAC, a regression analysis of the database consisting of the results of the 18 specimens that were experimentally tested and the 44 specimens that were numerically analyzed was carried out by considering the following parameters: compressive strength of RAC, steel bar size, anchorage length, and concrete cover. Based on the behavior of the variables in the parametric study (Subsection 4.4), the bond strength formula can take the following form:

$$\tau = C\,(f_c)^{K1} * \left(\frac{c^{k2}}{d_b * l_b}\right) \tag{2}$$

where τ is the bond strength of RAC; C is a statistical constant chosen to make the proposed numerical bond strength equal to 1.0; fc is the compressive strength of RAC; c is concrete cover; db is the diameter of the reinforcing bar; and lb is the embedded length in the RAC specimen. According to the parametric study, the compressive strength of RAC has a power function of 0.57; the bar diameter and the embedded length have a linear proportional function; finally, the concrete cover has a power function of 0.03. Thus, the final form of the proposed design equation is:

$$\tau = 2530\,(f_c)^{0.57} * \left(\frac{c^{0.03}}{d_b * l_b}\right) \tag{3}$$

6 Verification of the Proposed Equation

From Figure 9 and Table 6, the average ratio between the proposed (Eq. 3) and numerical (Subsection 4.4) bond strength of the reinforcing rebar in RAC is 0.98 and R-squared is 0.96. Also, From Figure 10 and Table 7, the average ratio between the proposed (Eq. 2) and experimental bond strength is 0.98 and R-squared is 0.93. The high R-square values of the proposed equation prove the its accuracy by comparison with the numerical and experimental results.

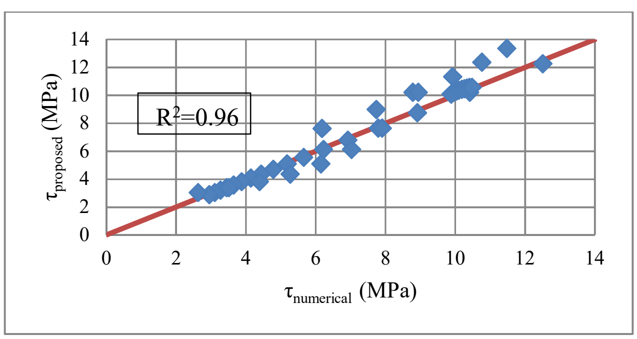

Figure 9 Numerical and proposed bond strength.

Table 6 Proposed and numerical bond strength**.**

No.	d_b (mm)	l_b (mm)	c (mm)	f_c (MPa)	$\tau_{numerical}$ (MPa)	$\tau_{proposed}$ (MPa)	τ_{pro}/τ_{num}
1	10	150	150	25	12.50	12.27	1.01
2	12	150	150	25	10.40	10.23	1.01
3	14	150	150	25	8.91	8.77	1.01
4	16	150	150	25	7.79	7.67	1.01
5	18	150	150	25	6.91	6.82	1.01
6	20	150	150	25	6.22	6.13	1.01
7	22	150	150	25	5.65	5.58	1.01
8	24	150	150	25	5.17	5.11	1.01
9	26	150	150	25	4.77	4.72	1.01
10	28	150	150	25	4.43	4.38	1.01
11	30	150	150	25	4.13	4.09	1.01
12	32	150	150	25	3.87	3.83	1.01
13	34	150	150	25	3.64	3.61	1.00
14	36	150	150	25	3.44	3.41	1.00
15	38	150	150	25	3.26	3.23	1.00
16	40	150	150	25	3.09	3.06	1.00
17	42	150	150	25	2.94	2.92	1.00
18	12	100	150	25	8.78	10.23	0.85
19	12	150	150	25	7.90	7.67	1.02
20	12	200	150	25	7.02	6.13	1.14
21	12	250	150	25	6.14	5.11	1.20
22	12	300	150	25	5.26	4.38	1.20
23	12	350	150	25	4.38	3.83	1.14
24	12	400	150	25	3.50	3.41	1.02
25	12	450	150	25	2.62	3.06	0.85
26	12	600	150	25	6.18	7.64	0.80
27	12	150	150	15	7.73	9.00	0.85
28	12	150	150	20	8.93	10.23	0.87
29	12	150	150	25	9.92	11.35	0.87
30	12	150	150	30	10.75	12.39	0.86
31	12	150	150	35	11.47	13.37	0.85
32	12	150	150	40	12.10	14.30	0.84
33	12	150	150	45	12.67	15.18	0.83
34	12	150	150	50	13.19	16.03	0.82
35	12	150	150	55	9.88	10.10	0.97
36	12	150	100	25	9.88	10.10	0.97
37	12	150	150	25	9.95	10.23	0.97
38	12	150	200	25	10.03	10.32	0.97
39	12	150	250	25	10.10	10.38	0.97
40	12	150	300	25	10.18	10.44	0.97
41	12	150	350	25	10.25	10.49	0.97
42	12	150	400	25	10.33	10.53	0.98
43	12	150	450	25	10.40	10.57	0.98
44	12	150	500	25	10.48	10.60	0.98
							Mean=0.98

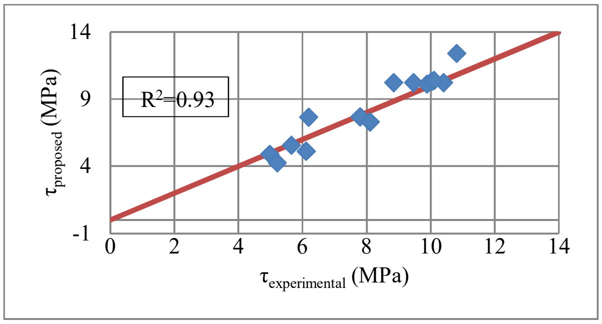

Figure 10 Experimental and proposed bond strength.

Table 7 Proposed and experimental bond strength.

Specimens	$\tau_{experimental}$ (MPa)	$\tau_{proposed}$ (MPa)	τ_{exp}/τ_{num}
B1-R50%	10.4	10.23	1.01
B2-Rep50%	11.12	10.23	1.08
B3-Rep0%	11.96	10.23	1.16
B4-fc15	6.18	7.64	0.80
B5-fc35	10.81	12.39	0.87
B6-fc50	12.67	15.18	0.83
B7-D16	7.79	7.67	1.01
B8-D22	5.65	5.58	1.01
B9-D25	4.97	4.91	1.01
B10-Em7 D	8.11	7.30	1.10
B11-Em10 D	6.11	5.11	1.19
B12-Em12 D	5.21	4.26	1.22
B16-Co100	9.88	10.10	0.97
B17-Co200	10.03	10.32	0.97
B18-Co250	10.1	10.38	0.97
			Mean=0.98

7 Conclusion

Experimental and numerical investigations were performed to evaluate the bond strength between reinforcing bar and surrounding RAC. Based on the results obtained from this study, the following conclusions can be drawn:

1. The bond strength of concrete is reduced by 13% when using a specimen constructed from recycled aggregate compared with conventional concrete.
2. As in the case of conventional concrete, when increasing the compressive strength of the RAC, the yield stress of the steel bar and the concrete cover, the bond strength increases. Meanwhile, when increasing the embedded length and the size of the rebar, the bond strength decreases.

3. The bond stress-slip behavior of the RAC is similar to that of conventional strength concrete.
4. The modes of failure of the reinforcing bar embedded in RAC are splitting failure and push-out failure, similar to conventional concrete.
5. The bond strength in RAC is related to a 0.57 power function with the compressive strength of RAC.
6. The proposed design equation to predict the bond strength of RAC was presented and compared with the experimental and numerical results. It was shown that the equation has a good accuracy.

8 Recommendation for Future Studies

Future studies should investigate the effect of the rib properties of deformed bars on the on bond strength of RAC. Further, the effect of the RAC replacement ratio should be included in the proposed equation of bond strength of RAC.

References

[1] Tayeh, B.A., Al Saffar, D.M. & Alyousef, R.A., *The Utilization of Recycled Aggregate in High Performance Concrete: A Review*, Journal of Materials Research and Technology, **9**(4), 84-89, 2020.

[2] Arafa, M.A., Tayeh, B.A., Alqedra, M.S., Shihada, S.A. & Hanoona, H. A., *Investigating the Effect of Sulfate Attack on Compressive Strength of Recycled Aggregate Concrete*, Journal of Engineering Research and Technology, **4**(4), pp. 20-25, 2017.

[3] Tayeh B.A., Shihada S.M. & Yusuf M.O., *Pull-out Behavior of Post Installed Rebar Connections Using Chemical Adhesives and Cement Based Binders*, Journal of King Saud University-Engineering Sciences, 1-31, **3**(4), pp. 1-3, 2019.

[4] Mohammed A.B., Rita N.M. & Bassam A.T., *Properties of Self-compacting High-strength Concrete Containing Multiple Use of Recycled Aggregate*, Journal of King Saud University – Engineering Sciences, **2**(32), pp. 198-114, 2020.

[5] Alhawat M.A. & Ashour A.B., *Bond Strength between Corroded Steel Reinforcement and Recycled Aggregate Concrete*, Structures, Structures, **19**(1) pp. 369-385, 2019.

[6] Arezoumandi M.A., Amanda R.B. & Jeffery S.M., *Evaluation of the Bond Strengths between Concrete and Reinforcement as a Function of Recycled Concrete Aggregate Replacement Level,* Structures, **18**(1), pp. 1-39, 2018.

[7] Butler L.B., West J.N. & Tighe, S., *The Effect of Recycled Concrete Aggregate Properties on the Bond Strength between RCA Concrete and Steel Reinforcement*, Cement and Concrete Research, **41**(1), pp. 1037-1049, 2011.

[8] Dong H.B., Song Y.V., Wanlin C.L., Wenjuan S.C. & Jianwei Z.B., *Flexural Bond Behavior of Reinforced Recycled Aggregate Concrete*, Construction and Building Materials, **2**(13), pp. 514-527, 2019.
[9] Fernandez I.C., Etxeberria M.H. & Marí A.X., *Ultimate Bond Strength Assessment of Uncorroded and Corroded Reinforced Recycled Aggregate concretes*, Construction and Building Materials, **1**(11), pp. 543–555, 2016.
[10] Kim S.Z., Yun H.V., Park W.G. & Jang Y.N., *Bond Strength Prediction for Deformed Steel Rebar Embedded in Recycled Coarse Aggregate Concrete*, Materials & Design, **8**(3), pp. 257-269, 2015.
[11] Pandurangan K.A., Dayanithy A. & Prakash O.D., *Influence of Treatment Methods on the Bond Strength of Recycled Aggregate Concrete,* Construction and Building Materials, **12**(1), pp. 212–221, 2016.
[12] Prince M.C., Gaurav G.A. & Singh B.S., *Splice Strength of Steel Reinforcement Embedded in Recycled Aggregate Concrete*, Construction and Building Materials, **1**(4), pp. 156-168, 2018.
[13] Bilal S.X., Hamad D.A. & Ghassan R.A., *Studies of the Effect of Recycled Aggregate on Flexural, Shear, and Bond, Splitting Beam Structural Behavior*, Case Studies in Construction Materials **9**(1), pp. 112-136, 2018.
[14] Pour M.S. & Alam M.C., *Investigation of Compressive Bond Behavior of Steel Rebar Embedded in Concrete with Partial Recycled Aggregate Replacement*, Structures **12**(4), pp. 105-117, 2016.
[15] ASTM C33-13*: Standard Specification for Concrete Aggregates,* 2013.
[16] RILEM/CEB/FIP *Recommendations on Reinforcement Steel for Reinforced Concrete*, (RC 6, CEB News 73), 1983.
[17] Simulia, Abaqus/CAE User's Manual, Version 6.14, 2016.
[18] Al-Quraishi H.A., Mohammed J.A. & Nada S.A., *A New Shear Strength Model for UHPC Corbel*, International Review of Civil Engineering, **9**(4), pp. 168-173, 2018.
[19] Al-Quraishi H.A., Al-Farttoosi M.H. & AbdulKhudhur R.A., *Tension Lap Splice Length of Reinforcing Bars Embedded in Reactive Powder Concrete (RPC).* Structures, **19**(1), pp. 362-368, 2019.